Quantum Interference Effects in the Ultraviolet Photolysis of Ar−HCl Following Partial Fragmentation into H + Ar−Cl

J. C. Juanes-Marcos and A. García-Vela*

Instituto de Matemáticas y Física Fundamental, C.S.I.C., Serrano 123, 28006 Madrid, Spain

Received: September 25, 2001; In Final Form: November 1, 2001

The fragmentation dynamics of Ar−HCl following ultraviolet photoexcitation is studied both classically and by an exact wave packet calculation. The focus of the analysis is on the partial fragmentation pathway Ar−HCl + $h\nu \rightarrow$ H + Ar−Cl. The results suggest that there is a competition between two different and simultaneous dissociation mechanisms of hydrogen, namely, direct dissociation and indirect dissociation involving a collision between H and Ar. These two dissociation mechanisms populate different states of partial fragmentation and total fragmentation (into H + Ar + Cl), which interfere upon the H/Ar collision. A global interpretation of the photolysis process based on the interference between the two types of dissociation and consistent with all the quantum results found is proposed. Such an interpretation appears to be general for the UV photolysis of a wide variety of hydrogen-bonded clusters. A means to control the interference mechanism in order to enhance the yield of a specific fragmentation pathway is suggested.

I. Introduction

In the last years an increasing attention has been devoted to the ultraviolet (UV) photodissociation of weakly bound hydrogen-bonded clusters of the type Rg_n−HX, $(HX)_n$, and Rg_n−H_2Y (X = halogen, Rg = rare gas, Y = O, S), both experimentally[1−9] and theoretically.[10−27] One of the main motivations is the possibility of investigating in these small systems, with one or a few solvent atoms, solvation effects typical of condensed matter environments. An advantage of these systems is the restricted range of initial relative geometries of the weakly bound species imposed by the cluster geometry.[28−32] As a consequence, the reaction dynamics started from the cluster samples a smaller volume of phase space as compared with the full collision situation, simplifying the analysis of the problem.

A few years ago a new and interesting possibility for the UV photodissociation of hydrogen-bonded clusters was suggested by Wittig and co-workers[2]: the preparation of open-shell complexes as products of the cluster photolysis. These authors studied the UV photolysis of the Ar−HI cluster by means of energy-resolved experiments.[2] They measured the time-of-flight (TOF) spectrum of the H fragment using a high-*n* Rydberg TOF (HRTOF) spectroscopic technique, and found a blue shift in the hydrogen kinetic-energy release distribution obtained from the TOF spectrum. Such an energy gain of some hydrogen fragments was interpreted as an indirect evidence that bound Ar−I radical complexes were produced in the photolysis. The HRTOF technique was also applied to investigate the UV photolysis of hydrogen-bonded clusters such as $(HI)_2$[3] and $(HCl)_2$,[4] and evidence of formation of I−HI and Cl−HCl radicals, respectively, was observed.

Recent experiments by Nesbitt and co-workers on the photolysis of Ar_n−H_2S ($n \leq 2$) precursors,[7] carried out at two different wavelengths, 248 nm and 193 nm, provided the first direct observation of Ar−SH and Ar_2−SH open-shell complexes from laser-induced fluorescence (LIF) spectra. A high efficiency of radical formation was found for excitation at 248 nm (15%), while it decreased to 10-fold lower when photolysis was carried out at 193 nm. The authors proposed a "gentle recoil" mechanism[7] to explain their experimental results. This mechanism is based on the fact that the recoiling H fragment carries most of the excitation energy initially deposited in the cluster, leaving only a small fraction of this energy to be accommodated in the radical formed. By increasing the excitation energy, the fraction of energy available for the radical increases correspondingly, leading to a decrease of the percentage of surviving radicals.

All the above experimental information indicates that there is a variety of small hydrogen-bonded clusters from which different radical complexes can be prepared upon UV photolysis. Formation of radical products has been studied theoretically in the case of UV photodissociation of the Ar−HCl precursor.[16,19] Upon UV photolysis Ar−HCl can follow two possible fragmentation pathways. One pathway implies total fragmentation (TF) of the cluster, Ar−HCl + $h\nu \rightarrow$ H + Ar + Cl, and it was found to dominate the photodissociation process at most of the excitation energies in the range of the absorption spectrum of Ar−HCl. Total fragmentation typically involves (at least) one collision of the departing hydrogen with Ar, through which energy is transferred to the Ar−Cl bond and breaks it. The other pathway is partial fragmentation (PF) into H and Ar−Cl radicals. The mechanism involved in this case is a direct dissociation of the hydrogen without interaction with Ar.

Energy-resolved probabilities of formation of Ar−Cl were reported for several excitation energies of the parent cluster in the region covered by the absorption spectrum.[19] A global yield of Ar−Cl production of 1.1% of the photodissociation process was found in the whole range of energies studied. The most interesting finding was a strong dependence on the excitation energy of both the percentage of the pathway of Ar−Cl formation, and the final state distributions of the radical products. Production of Ar−Cl was found to be the dominant pathway at very low excitation energies, then decreasing sharply with energy up to reaching a percentage of about 1%, which remains rather stable for medium or even high excitation energies. For very high energies an unexpected increase in the percentage of Ar−Cl formation was found. Further calculations showed that

10.1021/jp0136213 CCC: $22.00
Published on Web 12/08/2001

such an increase was artificial, due to nonconverged results at very high energies. Converged fragment distributions have been reported in an Erratum.[19b] The new results show that the percentage of Ar−Cl production decays monotonically with the excitation energy, which agrees with the trend observed experimentally for photolysis of Ar_n-H_2S ($n \leq 2$) clusters at two different wavelengths.[7] This is consistent with the gentle recoil mechanism suggested by Nesbitt and co-workers. However, some of the previous results cannot be explained only in terms of such a direct dissociation mechanism.

The converged fragment distributions present new features which suggest the existence of effects of quantum interference between the states populated by the two fragmentation pathways. To confirm such a hypothesis new quantum mechanical fragment distributions have been calculated and compared to classical ones. A global interpretation of the photolysis process consistent with the previous and present results and involving a mechanism of interference between states populated by the TF and PF pathways is suggested for the first time. Such an interpretation could be applicable to the UV photolysis of a wide variety of hydrogen-bonded clusters.

The paper is organized as follows. In Section II the methodology used is briefly outlined. The results are presented and discussed in Section III. Some conclusions are drawn in Section IV.

II. Methodology

The procedure applied to obtain the quantum mechanical energy-resolved state distributions of the photofragments consists of two steps. In a first step the UV photolysis of Ar−HCl is simulated with an exact 3D wave packet propagation method, which was previously described.[16,19a] The photolysis process occurs upon optical excitation of the HCl chromophore from its ground electronic state $X^1\Sigma^+$ to the repulsive excited state $A^1\Pi$. This excitation is simulated by promoting vertically the calculated vibrational ground state of the cluster[15,16] in the $X^1\Sigma^+$ potential surface to the excited $A^1\Pi$ surface, assuming a Franck−Condon transition. Such an ultrashort, δ-pulse excitation in time prepares an Ar−HCl wave packet in the upper surface which contains a broad band of energies. Details on the ground and excited potential surfaces have been given elsewhere.[15,16] The wave packet is propagated for a time $t_f = 80$ fs. The second step in our procedure consists of obtaining the energy-resolved fragment state distributions. To this purpose, the asymptotic wave packet is projected out onto the states of the products H + Ar−Cl corresponding to different total energies E of the parent cluster in the excited potential surface. The projection method has been already described.[19]

Classical fragment distributions are obtained after propagating classical trajectories for the same time as in the wave packet calculation. Initial conditions for the trajectories are sampled using the probability distribution associated with the initial wave packet. A sampling method recently suggested[33] has been applied where a quantum initial phase-space distribution is defined as $|\Phi\tilde{\Phi}|^2 f$. In this definition Φ and $\tilde{\Phi}$ are the initial state in coordinate and in momentum space, respectively, and f is the coordinate dependence of the volume element (in the Jacobi coordinates used $f = \sin\theta$, being θ the Jacobian angular coordinate; see ref 33 for details). A phase-space grid is then defined and initial conditions are sampled uniformly within that grid following the above distribution.

The initial conditions sampled are required to correspond with specific excitation energies E of the parent cluster in the upper potential surface, within an energy dispersion ΔE. This ensures that the classical fragment distributions calculated are energy-resolved and comparable to the quantum mechanical ones. In all calculations the energy dispersion of the initial conditions was $\Delta E = \pm 10$ cm^{-1}. The demanding criterion of such a small dispersion is required to obtain meaningful state distributions of the Ar−Cl fragment, since their energy domain is $\simeq 200$ cm^{-1}. Calculations were carried out for different excitation energies in the range of the absorption spectrum of Ar−HCl. More specifically, for energies $E = 1.55$ eV, 1.82 eV, 2.34 eV, 2.87 eV, 3.39 eV, 3.92 eV, and 4.97 eV, the number of trajectories integrated was 1183, 7519, 32229, 42867, 41264, 22674, and 6013, respectively. The number of initial conditions corresponding with a specific excitation energy is related to the probability given by the phase-space distribution for that energy.

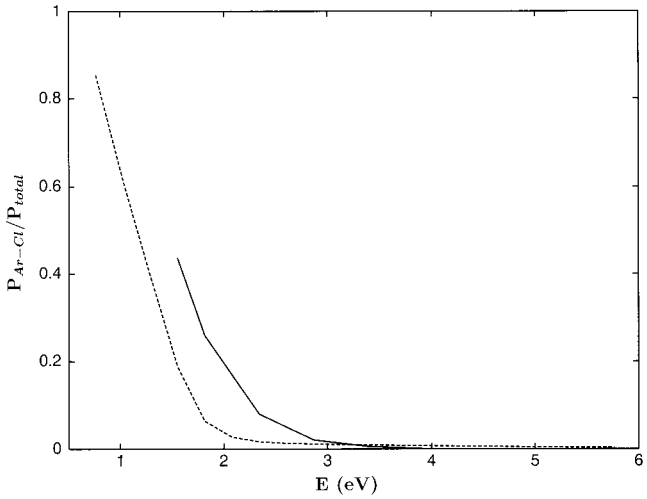

Figure 1. Ratio between the probability of Ar−Cl formation (P_{Ar-Cl}) and the total probability of photodissociation (P_{total}) vs E, calculated classically (solid line) and quantum mechanically (dashed line). The limit $E = 0$ corresponds to three separated atoms.

As pointed out above, partial fragmentation of Ar−HCl occurs through direct dissociation of the H fragment. For the cluster excitation energies studied this process is, in principle, expected to be rather classical in nature, and a classical description should be reasonably good. In this sense, significant deviations of the classical results from the quantum mechanical ones provide a probe of possible quantum effects, and in particular interference effects. In addition, a comparison of the quantum and classical predictions provides a test on the validity of the classical description of the PF pathway of this type of clusters upon UV photolysis.

III. Results and Discussion

A. Ar−Cl Fragment Distributions. As mentioned in the Introduction, some new features were found in the converged distributions reported in ref 19b which are relevant for the interpretation of the UV photolysis of Ar−HCl. In the following we shall discuss such features in combination with the new quantum and classical results reported here.

The behavior of the percentage of Ar−Cl formation, P_{Ar-Cl}/P_{total}, with the excitation energy E found in Figure 2b of ref 19b (shown in Figure 1) allows one to distinguish two main energy regions. One region is $E < 2.0$ eV, where P_{Ar-Cl}/P_{total} is nearly 1 at very low energies and decays sharply with increasing energy. The other region is $E > 2.0$ eV, where P_{Ar-Cl}/P_{total} keeps decaying but very slowly (in most of this region $P_{Ar-Cl}/P_{total} \approx 0.01$). The decreasing trend of P_{Ar-Cl}/P_{total} with increasing excitation energy would indicate that the gentle recoil

(or direct dissociation) mechanism of the hydrogen fragment would also operate in the photolysis of Ar−HCl, as expected.

However, there are two features in the distributions of Figure 2 of ref 19b which are difficult to explain only in terms of the gentle recoil mechanism. The first feature is related with the sharp decrease of P_{Ar-Cl}/P_{total} in the region $E < 2.0$ eV. It was discussed in ref 19a that for low excitation energies all the energy available for the radical can be accommodated as internal energy. Therefore, if P_{Ar-Cl}/P_{total} is governed only by the energy available for Ar−Cl after direct dissociation of H, it is surprising the sharp decrease found for this ratio for low energies E where still all the available energy can be absorbed by the radical.

The second feature has to do with the population of bound (P^b_{Ar-Cl}) and quasibound (P^q_{Ar-Cl}) states of Ar−Cl shown in Figure 2a of ref 19b. The quasibound states are supported by the rotational barrier $j(j+1)\hbar^2/2\mu_{r_{Ar-Cl}}(r_{Ar-Cl})^2$. As the energy available for the radical increases with increasing E, it is expected a gradual shift of the Ar−Cl population toward the energetically highest quasibound sltates, since these states can accommodate the largest amount of available energy. This implies that, except for very low energies, the population of quasibound states is expected to be higher than that of bound states. Indeed, for very low energies, $E < 1.0$ eV, $P^b_{Ar-Cl}(E) > P^q_{Ar-Cl}(E)$, and for 1.0 eV $< E <$ 2.3 eV, $P^q_{Ar-Cl}(E) > P^b_{Ar-Cl}(E)$, so up to $E \approx 2.3$ eV the expected trend is found. However, for $E > 2.3$ eV Figure 2a of ref 19b shows that the trend is inverted and $P^b_{Ar-Cl}(E) > P^q_{Ar-Cl}(E)$. This result is hard to interpret in terms of the effect of an increasing amount of available energy. A decrease of the population of quasibound states due to tunneling through the rotational barrier is unlikely. The time scale of tunneling decay of the quasibound states was analyzed by means of line-shape calculations.[19a,34] The decay lifetimes obtained (ranging from a few picoseconds to several tens of picoseconds) were much longer than the time scale of dissociation of the H fragment (a few tens of femtoseconds). Thus, the quasibound states can be considered as bound ones in practice.

In Figure 1 the quantum and classical behavior of P_{Ar-Cl}/P_{total} with the excitation energy is shown. The classical curve shows the same trend as the quantum mechanical one, decreasing with increasing excitation energy. Interestingly, the classical percentage of Ar−Cl formation is substantially higher than the quantum mechanical one for relatively low energies. The classical result is consistent with the behavior expected if the Ar−Cl formation is governed by the amount of energy available for the radical, as discussed above. Actually, in the classical description the Ar−Cl formation is governed essentially only by this available energy, therefore reflecting the outcome of the gentle recoil mechanism. Thus, the difference between the quantum and classical curves appears to be due to effects of quantum nature additional to that of the energy available for the radical.

The Ar−Cl ro-vibrational state distributions of Figure 3 of ref 19b show that the Ar−Cl radical complexes are produced with a high rotational excitation. This rotational excitation is explained in terms of the fragmentation mechanism which gives rise to Ar−Cl products. The radicals are produced by direct recoiling of H from initial Ar−HCl geometries where the hydrogen is not blocked by the Ar atom. These geometries imply large initial angles of the H−Cl bond with respect to the Ar−Cl internuclear axis, far from the equilibrium collinear configuration Ar···HCl. When the hydrogen recoils from these geometries, it produces a large torque on the Ar−Cl fragment, which excites the rotational mode.

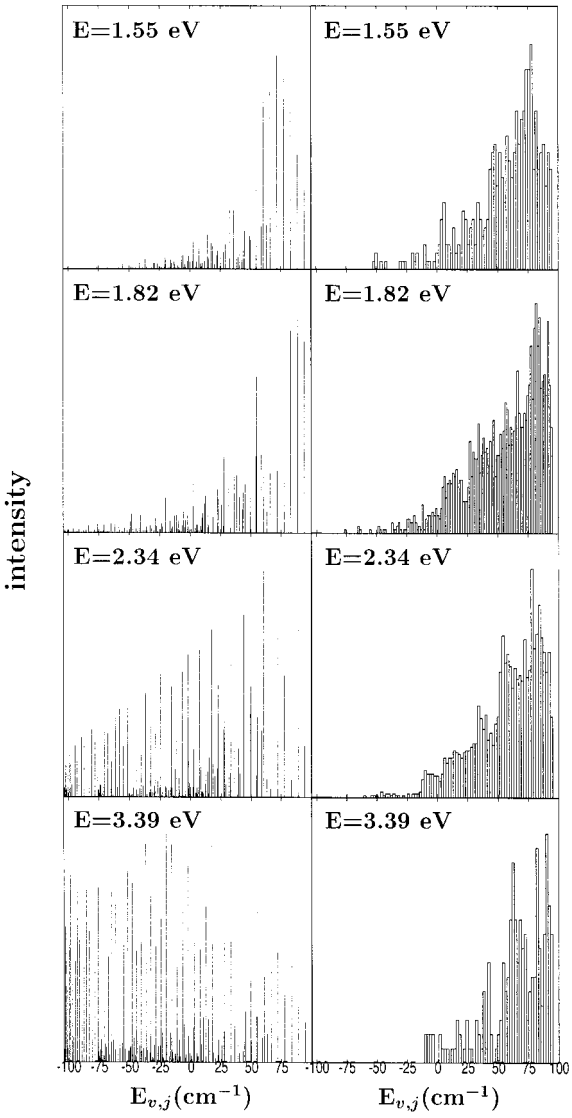

Figure 2. Internal energy distributions of the Ar−Cl radical for four different excitation energies calculated quantum mechanically (left panels) and classically (right panels). Normalization of the quantum and classical distributions is different.

It was found in Figure 3 of ref 19b that at very low excitation energies ($E < 2.0$ eV), as energy increases the population of Ar−Cl ro-vibrational states shifts gradually toward the energetically highest quasibound states. As already said, this is the expected behavior for a hydrogen direct fragmentation mechanism, where the probability of Ar−Cl formation is governed by the energy available for the radical (the gentle recoil mechanism). Consistent with the results of Figure 2a of ref 19b, about $E = 2.3$ eV the trend is inverted, and a gradual decrease of the population of quasibound states relative to the population of bound states is observed for $E > 2.3$ eV. We note that in the previous results of ref 19a this trend inversion was unclear, since in the nonconverged high-energy region of the distributions most of the radical population was localized in the highest quasibound states ($E_{v,j} > 50$ cm^{-1}). In contrast, the converged distributions show that for $E > 2.3$ eV the Ar−Cl radicals are produced dominantly in bound states.

Quantum and classical Ar−Cl ro-vibrational state distributions are shown in Figure 2 for different excitation energies. The above trend inversion is clearly observed in the quantum distributions, which also show that the population of quasibound states which decreases is mainly that of the energetically highest

ones. The decrease of the population of the highest quasibound states at medium and high energies is unexpected from a mechanism governed by an increasing amount of energy available for the radical. As E increases the recoiling hydrogen becomes more energetic, producing a larger torque on Ar−Cl and therefore a higher rotational excitation. Thus, the population of Ar−Cl should concentrate in the highest quasibound states, which correspond to the highest rotational states, and in addition can accommodate the largest amount of available energy, enhancing the survival probability of the radicals. Actually this is the behavior found in the classical distributions of Figure 2, which again are consistent with the trend expected for a PF pathway governed only by the energy available for the radical. We note the good agreement between the quantum and classical distributions for low excitation energies ($E \leq 1.82$ eV). This would indicate that the influence of the gentle recoil mechanism in the PF pathway is still large for low energies.

The results of Figures 1 and 2 seem to indicate that the energy available for the radical, and therefore the gentle recoil mechanism, is not the only factor governing the probability of Ar−Cl formation for different excitation energies. There appears to be some additional mechanism causing a decrease of population of the highest quasibound states as E increases. It is significant that both the sharp decrease of P_{Ar-Cl}/P_{total} at low energies, and the inversion of the expected trend of the population in bound and quasibound states, coincide with the increase of the probability of the TF pathway. In ref 19a it was suggested that the Ar−HCl photolysis is governed by a competition between the TF and PF pathways. It would be mainly this competition (along with the effect of the available energy) what determines the probability of radical formation. The purpose of the present work is to get deeper into such an interpretation, and to propose a more specific mechanism of photodissociation.

The j-state distributions of Figure 5 of ref 19b show a most interesting feature which is the gradual appearance of a structure as the excitation energy increases. For very low energies ($E <$ 1.5 eV) the structure is still weak, albeit noticeable, while for medium and high energies the structure is clearly apparent. The spacing between adjacent peaks of the structure is essentially constant within each j distribution. This spacing increases slowly (the number of peaks of the distribution decreases) as E increases. Actually the structure of the j distributions looks very much like a pattern of interference between different rotational states. Again the existence of such a pattern was unclear in the nonconverged distributions (see Figure 5 of ref 19a), due to the erratic behavior of the high-energy region of the distributions produced by the nonconvergence problems. Now the appearance of this pattern can be correlated with the gradual decrease of population in quasibound states, which provides new insight on the interpretation of the photolysis process.

Each distribution of Figure 5 of ref 19b is the sum of the rotational distributions corresponding to all the vibrational states of Ar−Cl. Analysis of the rotational distributions associated with each vibrational state of Ar−Cl provides interesting information on the origin of the structure shown by the distributions. In Figure 3 the rotational distributions of the three most populated vibrational states of Ar−Cl ($v = 0$, $v = 1$, and $v = 2$) are shown for four different excitation energies where the structure is clearly developed. For each energy the rotational distributions of $v = 0$, $v = 1$, and $v = 2$ present essentially the same pattern of peaks (the peak positions coincide). This common pattern is the one reflected in the j distributions of Figure 5 of ref 19b. The coherence in the structure of the three

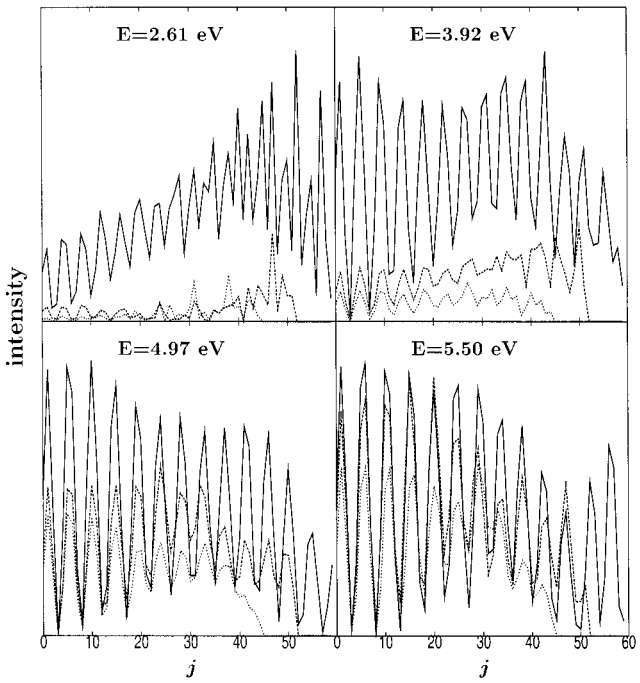

Figure 3. Rotational distributions of Ar−Cl associated with $v = 0$ (solid lines), $v = 1$ (dashed lines), and $v = 2$ (dotted lines) for four excitation energies.

rotational distributions suggests two implications. One implication is that interference between the Ar−Cl states is rather independent of the vibrational state of the radical. Interference occurs in a similar way for the different vibrational states, producing a similar pattern in the rotational distributions associated with each vibrational state. The other implication is that interference takes place mainly between Ar−Cl states with different j and the same v. This is not surprising since the couplings between states with different j are expected to be largest when v is conserved, due to the similar shape and nodal structure.

At very low energies ($E <$ 1.5 eV) the j distributions[19b] display a rather plain, continuous shape (except for the weak structure superimposed). Such a continuous shape is consistent with a radical production governed mainly by the energy available for the radical. As already pointed out, at low energies the Ar−Cl population shifts gradually toward the energetically highest states, also consistently with the effect of an increasing available energy for the Ar−Cl fragment. These results again seem to indicate that in the region of very low excitation energies, the probability of Ar−Cl formation and the specific shape of the ro-vibrational distribution of the radical is essentially determined by the amount of available energy.

An additional mechanism involving quantum interference between different states of the dissociating wave packet appears gradually with increasing excitation energy, and it competes with the effect of the available energy. The interference mechanism is already present at low energies, albeit weakly. In the region of medium and high excitation energies strong interference manifestations are found. As the intensity of the interference mechanism increases with increasing E, it produces two main effects on the Ar−Cl population. One is that the population of the highest quasibound states of Ar−Cl vanishes. The other effect is that the population distribution of surviving radicals develops a pronounced structure of peaks and nodes in the rotational quantum number. As a result, as energy increases the final state distributions of Ar−Cl become increasingly

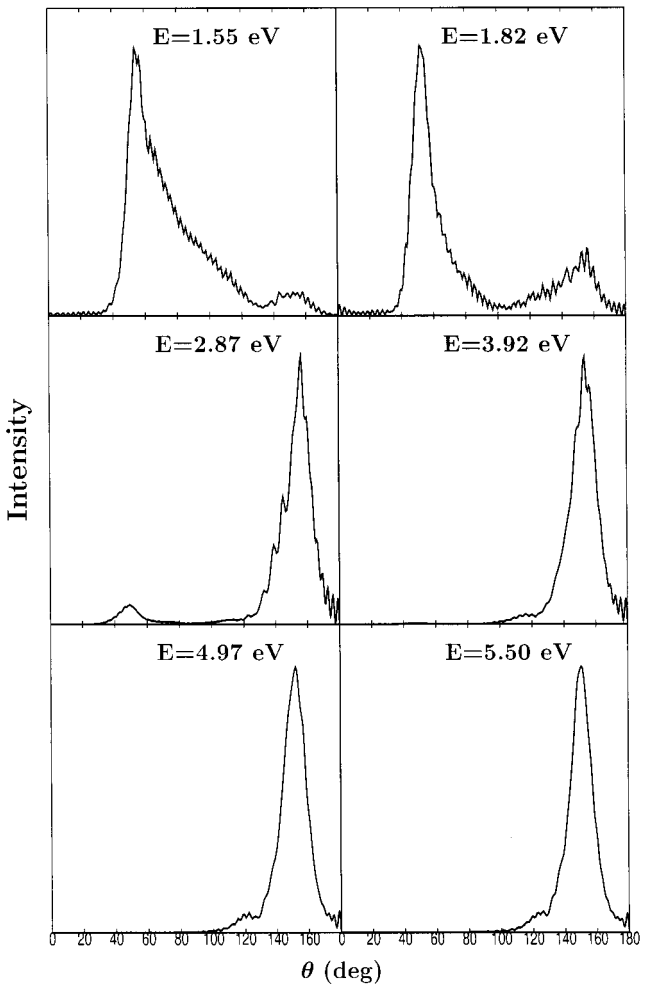

Figure 4. Quantum mechanical angular distributions of the H fragment for six excitation energies of Ar−HCl. The sin θ factor is included in the distributions.

different from those which would be produced only by the effect of the available energy (the classical distributions).

B. Angular Distributions of the H Fragment. The question rises about what is the origin and the specific mechanism which produces the manifestations of interference found in the quantum state distributions of the Ar−Cl radical. The angular distributions of the hydrogen fragment produced by the PF pathway provide the answer to this question. The quantum and classical angular distributions are shown in Figures 4 and 5, respectively for several excitation energies. The angle θ is that formed by the vectors associated with the Ar−Cl separation and the separation between H and the Ar−Cl center-of-mass, respectively. In the definition adopted here, $\theta = 0$ corresponds with the collinear configuration Ar−HCl, with the H position vector pointing toward the Ar atom.

The most interesting result of the quantum angular distributions is how their shape changes when E increases. For very low energies $E < 2.0$ eV the distributions are dominated by a broad peak centered around $\theta = 55°$. A small "bump" around $\theta = 155°$ is also displayed. With increasing excitation energy the peak at $\theta = 55°$ gradually disappears, reaching complete vanishing in the region $E > 3.4$ eV. The peak at large angles remains along the full energy range with a rather constant shape and relative intensity, and concentrates practically all the angular intensity for $E > 2.3$ eV. The vanishing intensity at relatively low and intermediate angles is mainly associated with the population of the highest quasibound states of Ar−Cl which

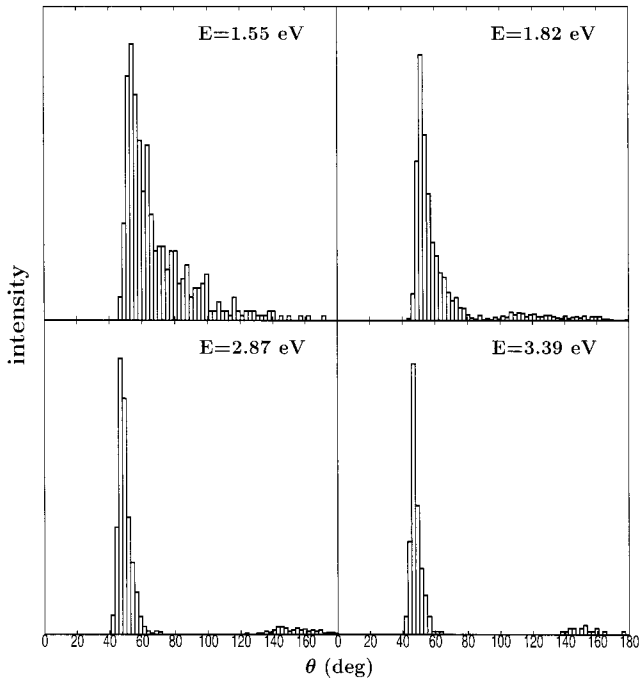

Figure 5. Classical angular distributions of the H fragment for four excitation energies of Ar−HCl.

gradually disappears with increasing energy. To a lesser extent the intensity in this angular region is also associated with vanishing population in Ar−Cl bound states. By contrast, the intensity at large angles is associated with the surviving population of Ar−Cl in bound (predominantly) and relatively low quasibound states.

Interestingly, the vanishing of the population in quasibound (and also bound) states occurs at low and intermediate angles, which is the region where the first collision between H and Ar takes place. This result suggests that the H/Ar collision is what causes the interference between the different wave packet states. Snapshots of the wave packet time evolution are shown in Figure 2 of ref 16. About $t = 10$ fs the wave packet collides with the Ar obstacle and breaks into three pieces. A small portion of the wave packet, composed only of TF states, remains in the interaction region for a while, chattering between Ar and Cl. The main part of the wave packet breaks into two pieces which travel toward the asymptotic region. These two pieces contain both TF and PF states which have interfered upon the collision.

Similarly as for the distributions of Figure 2, the classical distributions of Figure 5 agree reasonably well with the quantum mechanical ones for low energies ($E \leq 1.82$ eV), but clearly deviate from the quantum behavior as E increases. The classical distributions for energies $E > 2.0$ eV still display two peaks at the same positions as in the quantum distributions, but with the opposite intensities. The distributions of Figure 5 are consistent with the classical result that Ar−Cl is predominantly produced in quasibound states, mainly in the highest ones, and reflect the effect only of the energy available for the radical. The classical intensity remaining dominantly around $\theta = 50°$ as E increases, in contrast with the quantum result, would be due to the absence of interference effects in the classical description.

C. The Fragmentation Mechanism. In principle there are three possibilities of interference between wave packet states, namely interference between TF states themselves, interference between PF and TF states, and interference between PF states themselves. Here we shall focus on the interference between PF and TF states, and between PF states themselves, which is

the interference affecting the probability and state distributions of the Ar−Cl radicals formed.

Let us assume for a moment that the wave packet does not collide with the Ar obstacle. This would be the situation if the obstacle is small enough, such that the initial wave packet is not partially blocked. In this case the hydrogen would just recoil freely, leaving an amount of energy available for Ar−Cl which would depend on the excitation energy. As long as the available energy can be accommodated in the Ar−Cl radical, the products H + Ar−Cl would be dominant. For increasing available energy the radical population would shift toward the energetically highest states, and the Ar−Cl rotational distributions would be essentially unstructured. Actually this picture basically reflects what happens in the case of Ar−HCl photolysis for very low excitation energies. When the available energy would exceed the amount which can be absorbed by the radical, TF states (i.e., three-fragment or double-continuum states of Ar−HCl) would be populated. Since the H fragment carries most of the excitation energy, the energy available for the radical would be as much as a few hundreds of wavenumbers for the present range of excitation energies. Therefore the states populated in the Ar−Cl continuum spectrum would not lie very high in energy. The gradual increase of the energy available for Ar−Cl would give rise to a gradual decrease of the yield of radical formation (initially dominant).

The picture described above is consistent with the gentle recoil mechanism of Nesbitt and co-workers.[7] This picture can be considered as qualitatively valid to describe the actual Ar−HCl photolysis for the first few femtoseconds, before the H/Ar collision (actually as long as the hydrogen wave packet is far enough from Ar and the H−Ar interaction is still weak). Upon the H/Ar collision the situation changes drastically. Depending on the initial orientation of the hydrogen, the collision with Ar is harder or weaker, which determines the amount of energy transferred to the Ar−Cl bond. Such an energy transfer has the global effect of producing excitation of some of the population generated in PF states by direct dissociation of H in the beginning of the photolysis process (before the collision).

Indeed, population initially in PF (or single-continuum) states (with Ar−Cl either bound or quasibound) is excited and promoted to the double-continuum states of Ar−HCl upon the H/Ar collision. The quasibound PF states, and particularly the highest ones, are the most likely candidates to become double-continuum states, since they are already very excited and need only a small amount of energy to overcome the centrifugal barrier. This explains the vanishing of population in the highest quasibound states of Ar−Cl. As the excitation energy increases the energy transferred in the H/Ar collision increases as well, enhancing the probability of excitation of the quasibound population to the double-continuum states of Ar−HCl. Thus the population of quasibound states decreases with increasing E, consistently with the results found in the quantum mechanical Ar−Cl distributions. Population in bound PF states is also excited to TF states by the collision. However, excitation of the bound states is less likely than that of quasibound states, since it requires some more energy. As a consequence, the survival probability of Ar−Cl in bound states is higher than in quasibound states as E increases, which is reflected in the quantum results of Figure 2.

Interference between the PF and TF states of a given E, induced by the H/Ar collision, in combination with the effect of an increasing available energy for Ar−Cl with increasing E, is what determines the global yield of radical formation, $P_{Ar-Cl}(E)$, and the ratio $P_{Ar-Cl}(E)/P_{total}(E)$ for most of the excitation energies. Only at the lowest energies the effect of the energy available for the radical would be practically the only one present. The interference mechanism begins to operate at low energies, and causes a sharp decrease of $P_{Ar-Cl}(E)/P_{total}(E)$ up to about 4% in the region $E < 2$ eV, in contrast with the higher percentage found classically. For $E > 2$ eV the further decrease of $P_{Ar-Cl}(E)/P_{total}(E)$ is very slow, and the value of the ratio remains around 1% for most energies in this region. The angular distributions show that these radicals are produced by H direct dissociation at very large angles, far from the H/Ar collision region, which explains the robustness of this Ar−Cl population.

The H/Ar collision also induces interference between PF states themselves, which is largely responsible of the specific shape of the Ar−Cl state distributions. When the amount of energy transferred to Ar−Cl in the collision is small, only excitations between different PF states occur. This is the case of weak H/Ar collisions where the hydrogen recoils at rather large angles. Due to the large orientations, the collision between H and Ar produces a torque on the Ar−Cl fragment, and the energy is mainly transferred to the rotation of the radical. Thus, the collision-induced interference between different PF states involves essentially rotational rather than vibrational excitation of such states. This is in agreement with the low vibrational and high rotational excitation found in the radical state distributions. It also explains the pattern of interference of the Ar−Cl rotational distributions, and the result that this pattern is practically independent of the vibrational state of the radical (as seen in Figure 3). Actually, interference between PF states essentially means interference between the rotational states of Ar−Cl. As the energy transferred to Ar−Cl by weak collisions increases with E, the rotational transitions occur between states more separated in j, which explains the increase of the spacing between peaks in the j distributions of Figure 3.

We note that collision-induced interference between PF states involves excitation from bound to bound states, from bound to quasibound states, and from quasibound to quasibound states. Therefore, while the interference between PF and TF states causes vanishing of the population in some bound and quasibound states (particularly in the highest ones), such states can be populated again by the interference between PF states themselves. The final shape of the Ar−Cl state distributions is thus the result of the combined effect of the interference of the PF states with themselves and with the TF states.

In all the cases of interference between different states of the wave packet discussed above, it was assumed that in the collision the hot H fragment is the one which transfers energy to Ar−Cl. We believe that this is the most likely mechanism. However, there also exists the possibility that Ar−Cl transfers small amounts of energy to the hydrogen through weak collisions. Again such an energy transfer would involve mainly rotational transitions in Ar−Cl, but in this case going to a lower rotational state. Upon these rotational transitions only the quasibound PF states can interfere with the TF states associated with a lower rotational state. However, rotational deexcitation may also involve interference and transitions between PF states themselves, both bound and quasibound ones.

The fragmentation mechanism described above involving interference between different states of the cluster wave packet is consistent with all the quantum results found, and provides a global explanation of the Ar−HCl UV photolysis. Interference occurs between the states populated through two different dissociation mechanisms which take place simultaneously at the different excitation energies. One mechanism is direct dissocia-

tion of the hydrogen with no appreciable interaction with Ar. This mechanism populates both PF and TF states, depending on the energy available for the fragments. The other mechanism is an "indirect" or collision-mediated dissociation of H, and it populates mainly TF states (but also PF states if the collision is weak enough). Interference between the states populated by these two mechanisms depends on the couplings between them, but also on the initial population of such states, determined by the initial wave packet prepared by UV excitation of the cluster. We shall return to this point short below.

The mechanism of interference suggested to explain the Ar−HCl photolysis appears to be general for a wide family of hydrogen-bonded clusters. Indeed, there is a variety of hydrogen-bonded clusters which can meet the conditions for interference between different fragment states described in the above paragraph for Ar−HCl. In general these conditions imply simultaneous occurrence, at a given excitation energy, of the two hydrogen dissociation mechanisms, namely direct dissociation and collision-mediated dissociation, each of them producing different fragments (PF and TF states) which interfere. For clusters larger than triatomic ones, and depending on cluster size, there is a richer variety of possible fragments (i.e., of PF states), which will increase the possibilities of interference between fragment states. There is experimental evidence of radical formation upon UV photolysis (i.e., population of PF states leading to H and radical fragments through the direct dissociation mechanism), for different clusters such as Ar−HI,[2] $(HI)_2$,[3] $(HCl)_2$,[4] and Ar_n-H_2S ($n \leq 2$).[7] The other mechanism, collision-mediated dissociation of hydrogen, will occur as long as there is an obstacle to hydrogen recoil. This is a typical situation in hydrogen-bonded clusters, at least to a certain extent, due to the restricted range of initial intracluster geometries. Thus, the UV photolysis mechanism described here could be found in clusters of the families Rg_n-HX, Rg_m-H_2Y, and $(HX)_l$, with $n = 1$, $m = 1, 2$, and $l = 2$, and probably with $n > 1$ and $m, l > 2$, at least for small cluster sizes. Upon substitution of Rg by a molecular species (other than HX) like CO, CO_2, NO_2, C_2H_2, etc., the fragmentation mechanism is not expected to change.

A most interesting issue is the possibility of controlling the mechanism of interference in order to increase (or to decrease) the yield of a specific fragmentation pathway. As pointed out before, interference between fragment states depends on the initial population of such states prepared by UV excitation. Specifically, this initial population depends strongly on the cluster angular geometry distribution initially excited, since it determines the extent to which the hydrogen is blocked by the obstacle, and therefore the probability of the H/obstacle collision. Thus, selection of a cluster state with the desired geometry, prior to the UV pumping, provides a means to enhance a specific pathway.

An example is the Ar−HBr cluster, whose ground van der Waals (vdW) state for the $v = 0$ and $v = 1$ vibrational states of HBr corresponds with the isomer Ar−H−Br. However, the first vdW excited state with $v = 1$ is associated with the Ar−Br−H isomer.[35] The initial distribution of angular geometries associated with this vdW excited state, where the hydrogen is largely unblocked, would enhance the PF pathway. The possibility of controlling the yield of a specific fragmentation pathway through the distribution of cluster geometries initially excited, could also be explored in the framework of chemical reactions of the type $M-HX + h\nu \rightarrow H + MX$, with M = Li, Na, K, Ca.

IV. Conclusions

The UV photolysis of Ar−HCl is investigated by means of classical and exact 3D wave packet calculations. The focus is on the partial fragmentation pathway $Ar-HCl + h\nu \rightarrow H + Ar-Cl$. Energy-resolved distributions of the H and Ar−Cl radical fragments are analyzed in the energy range of the Ar−HCl absorption spectrum. The classical results for all excitation energies studied are consistent with a direct dissociation of the H fragment where the yield of Ar−Cl formation depends only on the energy available for the radical. The good qualitative agreement between the quantum and classical distributions for low energies indicates that in this energy range the effect of the available energy would be practically the only one governing the formation of Ar−Cl. With increasing excitation energy substantial differences appear between the quantum and classical predictions. Already at low energies an additional mechanism of quantum nature begins to operate, which competes with the effect of the available energy. This mechanism produces clear interference manifestations in the radical state distributions, and in particular in the rotational distributions.

Such a mechanism is identified as an indirect dissociation of the hydrogen fragment which, when recoiling, collides with the Ar atom. Upon this H/Ar collision the states associated with the different photolysis fragments (H + Ar−Cl and H + Ar + Cl in our case) interfere. An interpretation of the Ar−HCl fragmentation mechanism based on this collision-induced interference is suggested. This interpretation is consistent with and explains the behavior of all the quantum distributions calculated, providing the first global picture of the photolysis process. In this picture the Ar−HCl photofragmentation would be governed by the simultaneous occurrence and interference of two hydrogen dissociation mechanisms, direct dissociation and collision-mediated dissociation, each of them populating different states of the two fragmentation pathways. An implication is that the Ar atom, which acts as an obstacle to hydrogen dissociation and is far from being an spectator in the process, would be the origin of the interference mechanism. The present interpretation of the UV photolysis could be applicable to a wide variety of hydrogen-bonded clusters for which the above two types of H dissociation may occur.

Finally, a possibility is suggested to control the mechanism of interference such that the yield of a specific pathway is enhanced. It is based on the dependence of the outcome of interference between fragment states on the distribution of intracluster orientations initially excited. Thus, the photolysis process can be channeled toward the desired pathway by selecting a cluster state with the proper angular geometry, prior to the UV excitation.

Acknowledgment. This work was supported by D.G.I.C.Y.T., Spain, Grant No. PB95-0071, and by the EU network TMR Grant No. HPRN-CT-1999-00005.

References and Notes

(1) Segall, J.; Wen, Y.; Singer, R.; Wittig, C.; García-Vela, A.; Gerber, R. B. *Chem. Phys. Lett.* **1993**, *207*, 504.
(2) Jaques, C.; Valachovic, L.; Ionov, S.; Wen, Y.; Böhmer, E.; Segall, J.; Wittig, C. *J. Chem. Soc., Faraday Trans.* **1993**, *89*, 1419.
(3) Zhang, J.; Dulligan, M.; Segall, J.; Wen, Y.; Wittig, C. *J. Phys. Chem.* **1995**, *99*, 13680.
(4) Liu, K.; Kolessov, A.; Partin, J. W.; Bezel, I.; Wittig, C. *Chem. Phys. Lett* **1999**, *299*, 374.
(5) Young, M. A. *J. Chem. Phys.* **1995**, *102*, 7925.
(6) Plusquellic, D. F.; Votava, O.; Nesbitt, D. J. *J. Chem. Phys.* **1994**, *101*, 6356.
(7) Mackenzie, S. R.; Votava, O.; Fair, J. R.; Nesbitt, D. J. *J. Chem. Phys.* **1996**, *105*, 11360. *ibid.* **1999**, *110*, 5149.
(8) Votava, O.; Plusquellic, D. F.; Myers, T. L.; Nesbitt, D. J. *J. Chem. Phys.* **2000**, *112*, 7449.
(9) Baumfalk, R.; Buck, U.; Frischkorn, C.; Nahler, N. H.; Hüwel, L. *J. Chem. Phys.* **1999**, *111*, 2595.
(10) Alimi, R.; Gerber, R. B. *Phys. Rev. Lett.* **1990**, *64*, 1453.

(11) García-Vela, A.; Gerber, R. B.; Valentini, J. *J. Chem. Phys. Lett*. **1991**, *186*, 223. *J. Chem. Phys.* **1992**, *97*, 3297.
(12) García-Vela, A.; Gerber, R. B. *J. Chem. Phys.* **1993**, *98*, 427.
(13) García-Vela, A.; Gerber, R. B.; Imre, D. G.; Valentini, J. *J. Phys. Rev. Lett.* **1993**, *71*, 931.
(14) Schröder, T.; Schinke, R.; Mandziuk, M.; Bačić, Z. *J. Chem. Phys.* **1994**, *100*, 7239. Schröder, T.; Schinke, R.; Bačić, Z. *Chem. Phys. Lett.* **1995**, *235*, 316.
(15) García-Vela, A.; Gerber, R. B. *J. Chem. Phys*. **1995**, *103*, 3463.
(16) García-Vela, A. *J. Chem. Phys.* **1998**, *108*, 5755.
(17) Narevicius, E.; Moiseyev, N. *Chem. Phys. Lett.* **1998**, *287*, 250. *Mol. Phys*. **1998**, *94*, 897.
(18) Juanes-Marcos, J. C.; García-Vela, A. *J. Chem. Phys.* **1999**, *111*, 2606.
(19) (a) Juanes-Marcos, J. C.; García-Vela, A. *J. Chem. Phys.* **2000**, *112*, 4983. (b) *ibid.* **2001**, *115*, 5692 (E).
(20) Monnerville, M.; Pouilly, B. *Chem. Phys. Lett.* **1998**, *294*, 473.
(21) McCoy, A. B.; Hurwitz, Y.; Gerber, R. B. *J. Phys. Chem.* **1993**, *97*, 12516.
(22) Christoffel, K. M.; Bowman, J. M. *J. Chem. Phys.* **1996**, *104*, 8348.
(23) García-Vela, A.; Gerber, R. B.; Buck, U. *J. Phys. Chem.* **1994**, *98*, 3518.
(24) Schröder, T.; Schinke, R.; Liu, S.; Bacić, Z.; Moskowitz, J. W. *J. Chem. Phys.* **1995**, *103*, 9228.
(25) Niv, M. Y.; Krylov, A. I.; Gerber, R. B. *Faraday Discuss*. **1997**, *108*, 243. Niv, M. Y.; Krylov, A. I.; Gerber, R. B.; Buck, U. *J. Chem. Phys.* **1999**, *110*, 11047.
(26) Žďánská, P.; Schmidt, B.; Jungwirth, P. *J. Chem. Phys*. **1999**, *110*, 6246.
(27) Žďánská, P.; Slavíček, P.; Jungwirth, P. *J. Chem. Phys.* **2000**, *112*, 10761.
(28) Kleiber, P. D.; Lyyra, A. M.; Sando, K. M.; Zafiropulos, V.; Stwalley, W. C. *J. Chem. Phys.* **1986**, *85*, 5493.
(29) Wittig, C.; Radhakrishnan, G.; Buelow, S. *J. Chem. Phys*. **1986**, *84*, 727.
(30) Wittig, C.; Ionov, S.; Bruckner, G. A.; Jaques, C.; Valachovic, L. *J. Chem. Phys.* **1992**, *97*, 9486.
(31) Soep, B.; Breckenridge, W. H.; Jouvet, C. *J. Chem. Phys*. **1985**, *84*, 1443.
(32) Soep, B.; Krim, L.; Visticot, J. P. *J. Chem. Phys.* **1995**, *103*, 9589.
(33) García-Vela, A. *J. Chem. Phys.* **2000**, *112*, 8302.
(34) Halberstadt, N.; Beswick, J. A.; Janda, K. C. *J. Chem. Phys*. **1987**, *87*, 3966.
(35) Han, J.; McIntosh, A. L.; Wang, Z.; Lucchese, R. R.; Bevan, J. W. *Chem. Phys. Lett.* **1997**, *265*, 209.